MODELING OF INDUSTRIAL PSA PROCESS FOR FUEL ETHANOL PRODUCTION

Marian Simo, University at Buffalo, Buffalo, NY, USA
Christopher J. Brown, Thermal Kinetics Systems, Buffalo, NY, USA
and
Vladimir Hlavacek, University at Buffalo, Buffalo, NY, USA

Abstract

Dehydration of ethanol via adsorption on 3Å molecular sieves has recently been increasing in application in industry as an alternative to the conventional separation techniques for breaking the ethanol-water azeotrope. Over the past 20 years, Pressure-Vacuum Swing Adsorption (PSA) processes have gained increasing commercial acceptance as an energy-efficient separation technique. A general purpose package for simulation of cyclic adsorption processes based on the data from an operating plant and laboratory data has been developed. The dispersed plug flow model includes variation of axial velocity and the fluid flow follows Ergun‘s equation locally. A linear driving force mass-transfer-rate coefficient was used to describe adsorption and desorption kinetics. The operation of the column can be isothermal, adiabatic or non-isothermal non-adiabatic. The governing parabolic equations have been solved via method of lines using a stiff equation integration package. Several case study simulation results of dewatering the ethanol-water mixture in the fuel ethanol production process are presented.

Introduction

Previously, extractive or azeotropic distillation processes have been used to break the water-ethanol azeotrope [1]. Since distillation routes are energy intensive, attention has been paid to low energy separation alternatives such as liquid-liquid extraction, adsorption and membrane processes. Current industrial process prefers adsorption based dewatering of ethanol for large scale separations.

Ethanol can be produced by fermentation from practically any starch containing feedstock. Fermented liquor is distilled in the series of distillation columns including a stripping column, rectifying column, and in some processes a side stripper. To produce anhydrous ethanol, the water is removed with appropriately sized molecular sieve. 3Å zeolite materials are able to selectively adsorb water, due to the small size of their pores, while the ethanol molecules are excluded. The rectifying column is used to produce high ethanol content vapor, which is fed to Pressure-Vacuum Swing Adsorption (PSA) unit where ≥99.5 % (by weight) ethanol stream leaves the operation as final product. PSA process has proven to be much more energy efficient compared to classical process and now is commercially well-established as a separation process for dewatering the mixture of ethanol and water.

Precise design of PSA unit is a difficult task because of the many operational parameters characterizing this separation process. Laboratory scale experiments are time consuming and economically demanding. These reasons have led to the development of mathematical models which are used for initial evaluation of PSA process design and analysis.

PSA Simulation Model

The mathematical model describing a five-step PSA process involving high-pressure adsorption, blow-down, regeneration, purge and pressurization has been used in the present study for simulation of water-ethanol separation. A non-isothermal non-adiabatic dispersed plug flow model with variation of axial velocity has been used. The model assumes non-linear adsorption equilibrium. The mass transfer rate is described by the linear driving force (LDF) approximation. Based on assumptions of the adsorbing system, PSA bed models can be described by models having different levels of characterization of the system. Several transport effects, including the mechanisms of intra-particle diffusion and external mass transfer need to be considered. In our analysis, the LDF model was used as a compromise between accuracy and calculation efficiency [2]. The external mass transfer coefficient k_f was estimated from correlation given by Wakao [3].

Table 1. Summary of governing equations and simplifications

Mass balance for adsorbing component:	$\frac{\partial Y_1}{\partial t} = D_L \frac{\partial^2 Y_1}{\partial z^2} - \frac{u}{\varepsilon}\frac{\partial Y_1}{\partial z} - \frac{(1-\varepsilon)}{\varepsilon}\rho_s \frac{RT}{P}\frac{\partial q_1}{\partial t}(1-Y_1)$	(1)
Overall mass balance:	$\frac{1}{P}\frac{\partial P}{\partial t} - \frac{1}{T}\frac{\partial T}{\partial t} = -\frac{1}{\varepsilon}\frac{\partial u}{\partial z} - \frac{1}{\varepsilon}\frac{u}{P}\frac{\partial P}{\partial z} + \frac{1}{\varepsilon}\frac{u}{T}\frac{\partial T}{\partial z} - \frac{(1-\varepsilon)}{\varepsilon}\rho_s \frac{RT}{P}\sum_{n=1}^{n}\frac{\partial q_1}{\partial t}$	(2)
LDF rate:	$\frac{\partial q_1}{\partial t} = k_{LDF}(q_1^* - q_1) \quad \frac{1}{k_{LDF}} = \left[\frac{R_p}{3k_f} + \frac{{R_P}^2}{15\,\varepsilon_p\, D_{eff}}\right]\frac{q_1^*\rho_p}{C_i}$	(3, 4)
Energy balance:	$\left[\rho_g c_{p_g} + \frac{1-\varepsilon}{\varepsilon}\rho_s c_{p_s}\right]\frac{\partial T}{\partial t} = k_{ef}\frac{\partial^2 T}{\partial z^2} - \frac{u}{\varepsilon}\rho_g c_{p_g}\frac{\partial T}{\partial z} + (-\Delta H)\frac{(1-\varepsilon)}{\varepsilon}\rho_S \frac{\partial q_1}{\partial t} + \frac{4h}{D}(T - T_a)$	(5)
Ergun Equation (momentum balance):	$-\frac{dP(z)}{dz} = \frac{1-\varepsilon_b}{{\varepsilon_b}^3}\left(1.75 + \frac{150(1-\varepsilon_b)}{\mathrm{Re}_p(z)}\right)\frac{\rho_g w^2(z)}{d_p}$	(6)
Equilibrium:	$q_1^* = q_1^s \frac{K P_1}{1 + K P_1} \qquad \ln\left(\frac{K}{K_0}\right) = \frac{Q}{R}\left(\frac{1}{T} - \frac{1}{T_0}\right)$	(7, 8)
Simplifications:	1. Ethanol is inert (water is the only adsorbing component). 2. Local thermal equilibrium assumption – one-phase model. 3. Momentum balance follows quasi-steady state model. 4. Mass transfer mechanisms: external mass transfer and macro-pore diffusion. 5. Flow through valves is isentropic [4]. 6. Ideal gas equation of state for vapor phase.	

The value of tortuosity was considered to be 2 as reported in the work of Teo and Ruthven [5]. The value of effective thermal conductivity was estimated from correlation given by Votruba and Hlavacek [6]. The equilibrium data for 3Å molecular sieve adsorbent were provided by manufacturer.

The term representing the axial dispersion (equation 1) is very small compared to the convection term and equation 1 shows the properties of hyperbolic non-linear partial differential equation of the first order. However, the dispersion term eliminates the shock-like behavior and it is easier to solve these equations compared to those where the dispersion term is eliminated. The spatial discretization must be done carefully to suppress the numerical dispersion. The value of axial

dispersion coefficient D_L was calculated from the definition of longitudinal Peclet number for mass transfer. According to Froment [7], the Peclet number has a value of 2 if the ratio of the bed length to the particle diameter exceeds 50.

The system of governing equations was solved by using the initial and boundary conditions summarized in the *Table 2*. The PSA process simulation is always started from the adsorption step in all the simulations with a clean bed.

Table 2. Initial and Boundary conditions for governing equations

Cycle Step:			Note
I. Adsorption Step	$t = 0$	$\overline{Y} = \overline{q} = 0 \quad \overline{T} = T_a \quad \overline{P} = P_H$	1st cycle
		$\overline{Y} = \overline{Y}^{(V.)} \quad \overline{q} = \overline{q}^{(V.)} \quad \overline{T} = \overline{T}^{(V.)} \quad \overline{P} = \overline{P}^{(V.)}$	any other cycle
	$z = 0$	$Y = Y_F \quad T = T_F \quad u = u_F \quad P = P_H$	
	$z = L$	$\frac{\partial Y}{\partial z} = 0 \quad \frac{\partial T}{\partial z} = 0$	
II. 1st Depressurization	$t = 0$	$\overline{Y} = \overline{Y}^{(I.)} \quad \overline{q} = \overline{q}^{(I.)} \quad \overline{T} = \overline{T}^{(I.)} \quad \overline{P} = \overline{P}^{(I.)}$	any cycle
	$z = 0$	$\frac{\partial Y}{\partial z} = 0 \quad \frac{\partial T}{\partial z} = 0$	
	$z = L$	$\frac{\partial Y}{\partial z} = 0 \quad \frac{\partial T}{\partial z} = 0 \quad u = u(Valve)$	
III. 2nd Depressurization	$t = 0$	$\overline{Y} = \overline{Y}^{(II.)} \quad \overline{q} = \overline{q}^{(II.)} \quad \overline{T} = \overline{T}^{(II.)} \quad \overline{P} = \overline{P}^{(II.)}$	any cycle
	$z = 0$	$\frac{\partial Y}{\partial z} = 0 \quad \frac{\partial T}{\partial z} = 0$	
	$z = L$	$\frac{\partial Y}{\partial z} = 0 \quad \frac{\partial T}{\partial z} = 0 \quad u = u(Valve)$	
IV. Purge	$t = 0$	$\overline{Y} = \overline{Y}^{(III.)} \quad \overline{q} = \overline{q}^{(III.)} \quad \overline{T} = \overline{T}^{(III.)} \quad \overline{P} = \overline{P}^{(III.)}$	any cycle
	$z = 0$	$Y = Y_P \quad T = T_P \quad u = u_P$	
	$z = L$	$\frac{\partial Y}{\partial z} = 0 \quad \frac{\partial T}{\partial z} = 0 \quad P = P_L$	
V. Repressurization	$t = 0$	$\overline{Y} = \overline{Y}^{(IV.)} \quad \overline{q} = \overline{q}^{(IV.)} \quad \overline{T} = \overline{T}^{(IV.)} \quad \overline{P} = \overline{P}^{(IV.)}$	any cycle
	$z = 0$	$Y = Y_P \quad T = T_P$	
	$z = L$	$\frac{\partial Y}{\partial z} = 0 \quad \frac{\partial T}{\partial z} = 0 \quad u = u(Valve)$	

Solution of the governing equations

The governing equations reported in the *Table 1* represent a transient system of partial differential equations that typically have a steady state attractor. In the literature this attractor has been called "Cyclic Steady State" (CSS). However, owing to the highly non-linear behavior of the governing equations one can also expect multiplicity of CSS, oscillatory or chaotic behavior of the attractor. Stepanek [8] observed the multiple CSS, other types of attractors have not been determined so far.

There are several strategies to solve the PSA equations. The first strategy is based on the idea that the initial value problem for parabolic equations can be transformed to an elliptic problem where the missing boundary condition is the unknown CSS. After complete discretization both in time and space the algebraic non-linear equations can be solved by Newton-Raphson method. Nilchan [9] used

finite difference and collocation methods in both time and space to discretize the system of PDEs. This approach features several problems; among them are: huge dimension of the set on non-linear algebraic equations, formulation of the nominal initial guess for the Newton-Raphson method and failure to converge.

The second strategy is based on an appropriate approximation of the space operator by finite differences and the resulting set of ordinary non-linear stiff differential equations can be solved as an initial value problem by the method of lines (MOL). The advantage of this approach is that space and time discretization steps are decoupled; high-order accuracy can be achieved in each dimension. The spatial discretization can be achieved in a number of other ways. In addition to finite differences Galerkin finite element methods, orthogonal collocation, and finite volume approximation have been tested [10-12]. The steep adsorption fronts may cause significant numerical problems since the set of ODEs is stiff and anti-stiff integration routines must be used. To integrate these systems, integration packages such as LSODE, DASSL and DASPK, can be adopted.

In our calculations we have discretized the differential operator by the method of high-order difference scheme with the degree of approximation $O(h^4)$. Due to hyperbolic character of the problem the up-wind approximation has been used. The resulting system of ordinary differential equations was solved by a fourth-order Gear algorithm with a variable step size control strategy.

The simplest method of solution is a method of successive substitutions, sometimes also called Picard iteration method. This fixed point iteration is a reliable and stable technique and the convergence trajectory mirrors the actual physical transient of PSA process. In a case that certain eigenvalue of fixed point operator is close to the value 1 the governing equations can converge slowly.

In order to simplify and speed up the calculation of CSS, following simplification was used. Two time derivatives in the left hand side of (2) would lead to an implicit system of differential equations; numerical integration would then require solution of a system of algebraic equations at each integration step. The most convenient way to deal with problems like this is to approximate this equation according to a general formula:

$$[f(y)\times F(y)]^{n+1} \approx [f(y)]^{n} \times [F(y)]^{n+1} \tag{9}$$

Here f(y) represents the coefficients containing the dependent variable and F(y) is the linear differential operator. For reasonably short time steps the approximation results in differential equations with constant coefficients.

Case study

The annual ethanol production of the plant considered in the study is 55 million gallons. PSA unit consists of 2 beds filled with 3Å zeolite adsorbent. The operational parameters are summarized in *Table 3*.

The PSA cycle can be divided into following steps:

1. ***Adsorption (production) stage*.** The water-ethanol vapor stream is fed to the bed from the top at 55 psia pressure. At the bottom of the bed, the high pressure product stream is collected. Part of the product stream is used to re-pressurize and purge the bed during the desorption stage. The adsorption stage takes about 5.5 minutes.

2. ***Desorption stage*** follows after the production stage is completed. The bed must be depressurized, regenerated and re-pressurized to the original adsorption pressure.
   1st depressurization step: The pressure in the bed is 55 psia initially and declines to about 20 psia in 1 minute. The flow through the valve is critical during this stage, thus pressure decrease is linear. In our model, the rate of 1st depressurization is governed by the opening of the valve located at the top of the bed (counter-current depressurization). The vacuum level during this step is 5.5 psia.
   2nd depressurization step: The pressure at the outlet (top of the bed) is 20 psia and it declines exponentially to 2.0 psia in about 2.5 minutes. The vacuum applied during this step is decreased to 2.0 psia.
   Regeneration step with purge: The bed is purged using portion of the product stream. This step is very short in the plant, it takes only 15 seconds.
   Pressurization: Initially, the bed is under the desorption pressure – 2.0 psia and it is continually pressurized (from the bottom of bed) by the product stream all the way up to 55 psia in about 2 minutes.

Table 3. Summary of operational parameters

Feed gas:	
Composition - (Y_F)	0.182 (molar fraction of water)
Flowrate - (F_F)	20.41 metric tons/hr
Temperature - (T_F)	440 K
Production pressure - (P_H)	379212 Pa / 55 psia
Purge pressure - (P_L)	13790 Pa / 2 psia
Purge flowrate - (F_P)	1.36 metric tons/hr
Bed length - (L)	7.3 m
Bed diameter - (D)	2.4 m
Gas void fraction - (ε)	0.63
Bulk void fraction - (ε_b)	0.4
Heat of adsorption - (ΔH)	51.9 kJ/mol
Thermal capacity of gas - (C_{pg})	1000 J/kg/K
Thermal capacity of solid matrix - (C_{ps})	1260 J/kg/K
Effective thermal conductivity - (k_{ef})	41.26 W/m/K
Adsorbent-3Å molecular sieve:	
Bulk density - (ρ_b)	729 kg/m^3
Particle size (sphere diameter)	3 mm

Results and Discussion

Equations 1-8, the coupled partial differential and algebraic equations, were solved together with the initial and boundary conditions. The results have been obtained for 100 mesh points in the axial direction and a time step of 0.5 s. The CSS was reached after few hundreds of cycles, but never more than 1000 cycles. Average computational time for one cycle was approximately 30 seconds using a standard Dell Laptop Computer with 1.6 GHz processor.

Start-up of the Plant -Transient Phenomena.

The adsorption of water on the zeolite matrix is a strongly exothermic process and consequently there is no difference in qualitative behavior between start-up of a chemical reactor with an exothermic catalytic reaction with the Langmuir-Hinshelwood kinetic expression and an adsorber column used for dewatering of rich ethanol on zeolite adsorbent.

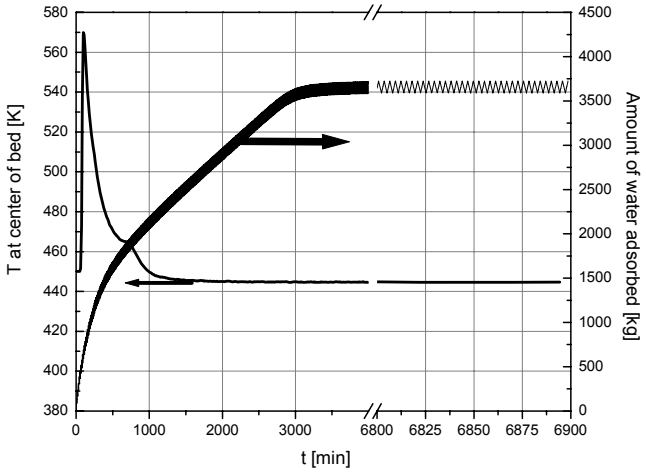

Fig.1: Transient start-up of the bed. Temperature in the center of the bed and the amount of water adsorbed in the bed is plotted against the operation time.

In *Fig. 1* we displayed the temperature at the geometrical center of the bed and the amount of water adsorbed in the bed. The simulation indicates that the initial temperature of bed T_i = 450 K increased to T=570 K in very short time after start-up. The strong temperature overshooting during the start-up of an exothermic catalytic reactor is well known fact and steps should be taken to avoid it or at least to lower it. The technical solution requires to start with pure ethanol as the feed stream and smoothly increase the concentration of water until required concentration of ethanol-water mixture is achieved. It is important to notice that the CSS is approached after 52 hours of operation. *Fig. 1* also reveals that the difference between the amount of water adsorbed and desorbed is constant at t > 3000 min., however the composition of product stream is constant after 4000 minutes of operation; see *Fig.2*.

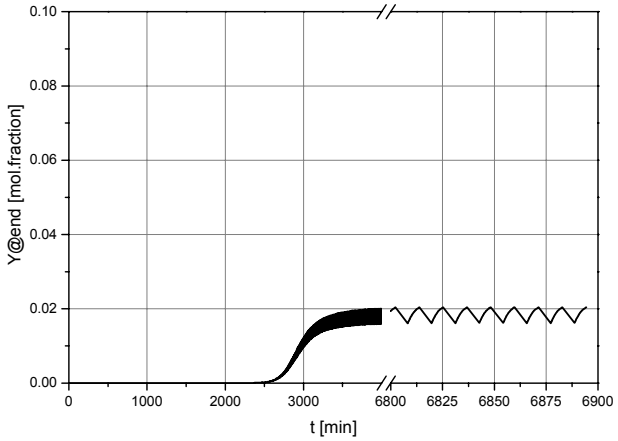

Fig.2: Molar fraction of water in product stream as a function of operation time during the start-up of

PSA unit.

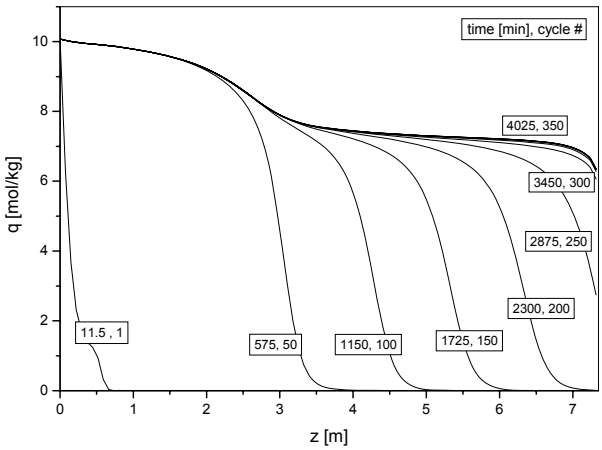

Fig.3: Solid phase-loading profiles of water as a function of operation time during the start-up of PSA unit plotted against bed axial coordinate. Axial coordinate at 0 m represents the top of the bed.

Fig. 3 shows the development of profiles in the solid phase as function of operational time and cycle number. It gives us better insight into the transient start-up of the PSA unit.

Qualitative behavior of the adsorption-desorption step.

Fig. 4 shows the development of the concentration profiles in the gaseous phase during the adsorption step after 600 cycles of operation. By this time the process has reached the CSS. We can notice that the concentration wave has all the properties of a constant pattern propagating wave, the exit concentration of ethanol is greater than 99.2 wt%. We can also observe that a major part of the adsorption bed (close to 50%) is poorly utilized.

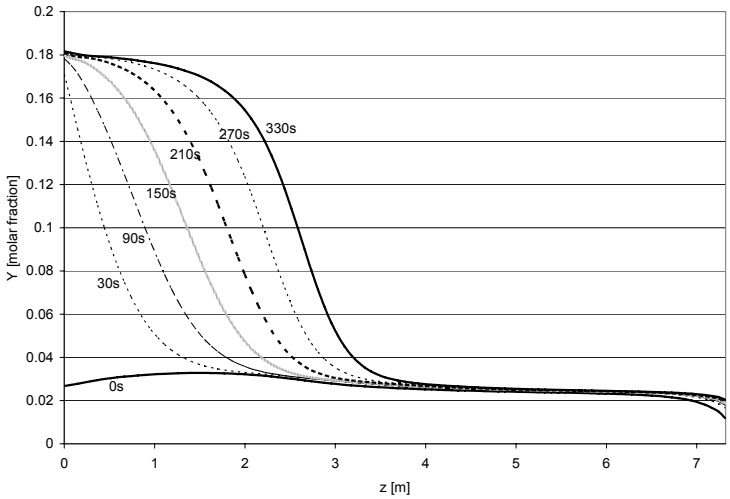

Fig.4: Water profiles in vapor phase of the bed during adsorption stage at CSS, 600 cycles. Axial coordinate at 0 m represents the top of the bed and flow direction is from top to bottom of bed.

Fig. 5 displays the development of the temperature profiles; we can notice that at the beginning the heat generated close to the adsorber inlet is conducted towards the cold internal part ($dT/dx < 0$); at $t \approx 150$ s the direction of the gradient is reversed and the heat propagates toward the inlet. A transient hot spot is produced and it moves in the direction of flow. The temperature profiles travel in the strip between two envelops and the temperature front is represented by a standing wave.

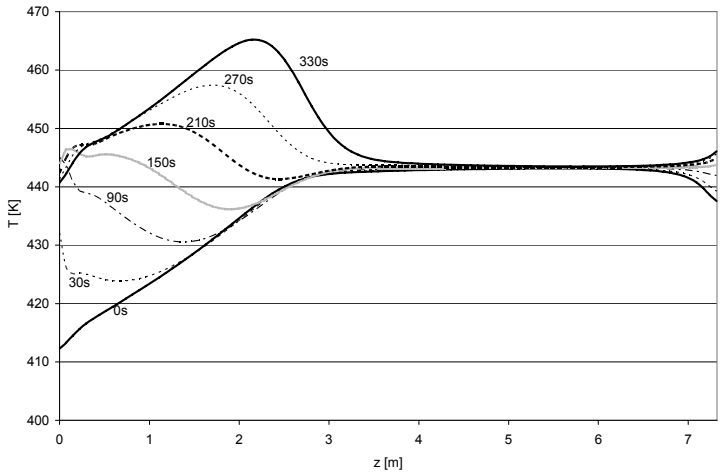

Fig.5: Temperature profiles in the bed during the adsorption stage at CSS, 600 cycles. Axial coordinate at 0 m represents the top of the bed and flow direction is from top to bottom of bed.

Upon decreasing the pressure in the adsorber; the partially saturated solid phase starts to release the adsorbed water and the concentration of the water in the gaseous phase increases. In the early stages of desorption the axial profiles of gaseous concentration of water are described by a standing wave (depressurization steps); cf. profiles for t=30 and 90s in *Fig. 6*.

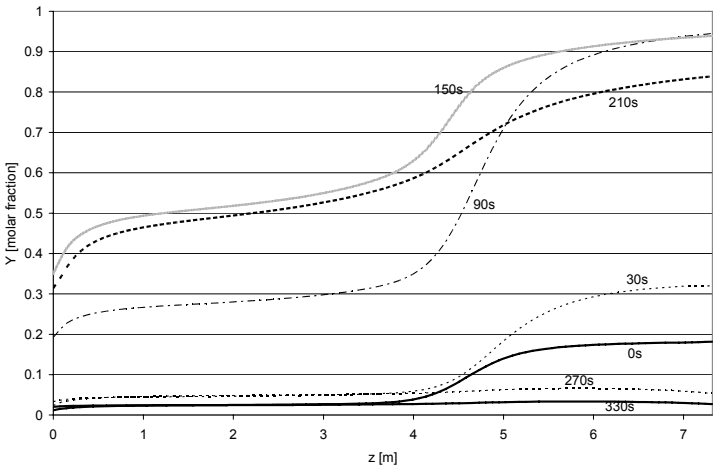

Fig.6: Water profiles in vapor phase of the bed during desorption stage at CSS, 600 cycles. Axial coordinate at 0 m represents the bottom of the bed and flow direction is from bottom to top of bed.

As a result of desorption taking place; the concentration in the solid phase decreases and the axial profiles of gaseous water concentration start to decrease as well, see profile 210s (regeneration step). At t = 330 sec, the bed is re-pressurized and the gaseous concentration is low.

Desorption is an endothermic process and as a result the temperature in the bed is dropping, *Fig. 7*. Again the temperature profiles move in the strip given by two envelops and the hot spot is eventually eliminated. In the area of the initial hot spot the temperature value decreases by almost 30 K. The internal temperature in the portion of the bed between z=0 and z=3.5 m stays constant during the desorption step, this portion represents bottom half of the bed since the flow is in the opposite direction compared to adsorption stage. Vapor flows from bottom of bed towards the top during desorption.

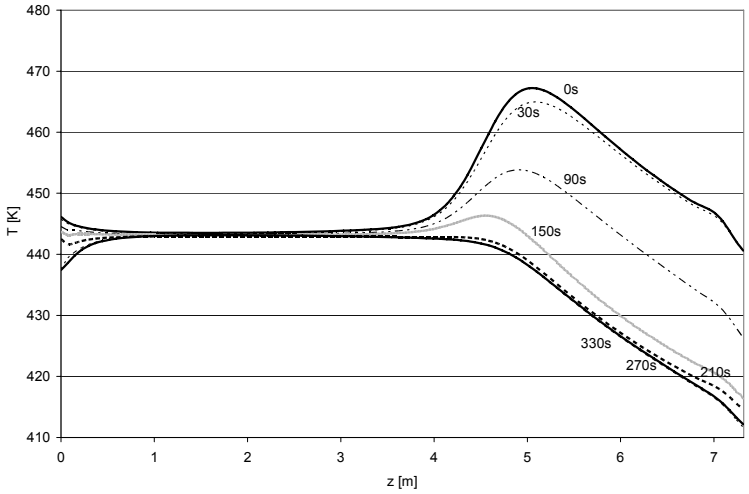

Fig.6: Temperature profiles in the bed during desorption stage at CSS, 600 cycles. Axial coordinate at 0 m represents the bottom of the bed and flow direction is from bottom to top of bed.

Conclusions & Future Work

A practically usable model for the calculation of transient start-up and CSS of the PSA process for fuel grade ethanol production has been developed and applied to a study of the process. Results obtained from the model have been compared with the plant data such as product composition, temperature and pressure profiles. The model has qualitatively described the operation of the industrial unit. We intend to use our program to investigate the effects of operational parameters and optimize the PSA cycle. Caution must be taken when applying the results because there is still opportunity for improvements in the program, including but not limited to inclusion of co-adsorption of ethanol and inclusion of experimentally verified mass transfer rates. Some of the simplifications we've applied here will be verified experimentally and necessary steps will be taken to incorporate them into the program.

References

1. Black, C., Distillation modeling of ethanol recovery and dehydration processes for ethanol and gasohol. Chemical Engineering Progress, 1980. 76(9): p. 78-85.
2. Gorbach, A., M. Stegmaier, and G. Eigenberger, Measurement and Modeling of Water Vapor Adsorption on Zeolite 4A-Equilibria and Kinetics. Adsorption, 2004. 10(1): p. 29-46.
3. Wakao, N. and T. Funazkri, Effect of fluid dispersion coefficients on particle-to-fluid mass transfer coefficients in packed beds. Correlation of Sherwood numbers. Chemical Engineering Science, 1978. 33(10): p. 1375-84.
4. Perry, R.H., Perry's Chemical Engineers' Handbook. 7th ed. 1997, New York: McGraw-Hill.
5. Teo, W.K. and D.M. Ruthven, Adsorption of water from aqueous ethanol using 3-.ANG. molecular sieves. Industrial & Engineering Chemistry Process Design and Development, 1986. 25(1): p. 17-21.
6. Votruba, J., V. Hlavacek, and M. Marek, Packed bed axial thermal conductivity. Chemical Engineering Science, 1972. 27(10): p. 1845-51.
7. Froment, F. and K.B. Bischoff, Chemical Reactor Analysis and Design. 2nd Ed. 1990. 664 pp.
8. Stepanek, F., et al., On the modeling of PSA cycles with hysteresis-dependent isotherms. Chemical Engineering Science, 1999. 55(2): p. 431-440.
9. Nilchan, S. and C.C. Pantelides, On the optimization of periodic adsorption processes. Adsorption, 1998. 4(2): p. 113-147.
10. Choong, T.S.Y., W.R. Paterson, and D.M. Scott, Development of novel algorithm features in the modeling of cyclic processes. Computers & Chemical Engineering, 2002. 26(1): p. 95-112.
11. Jiang, L., L.T. Biegler, and V.G. Fox, Simulation and optimization of pressure-swing adsorption systems for air separation. AIChE Journal, 2003. 49(5): p. 1140-1157.
12. Liu, Y., J. Delgado, and J.A. Ritter, Comparison of finite difference techniques for simulating pressure swing adsorption. Adsorption, 1998. 4(3 and 4): p. 337-344.